CD133$^+$ and CD133$^-$ Glioblastoma-Derived Cancer Stem Cells Show Differential Growth Characteristics and Molecular Profiles

Dagmar Beier,[1] Peter Hau,[1] Martin Proescholdt,[3] Annette Lohmeier,[1] Jörg Wischhusen,[5] Peter J. Oefner,[4] Ludwig Aigner,[2] Alexander Brawanski,[3] Ulrich Bogdahn,[1] and Christoph P. Beier[1]

[1]Laboratory of Neurooncology and [2]VW-Junior Group, Department of Neurology, [3]Department of Neurosurgery, and [4]Institute of Functional Genomics, University of Regensburg, Regensburg, Germany; and [5]Interdisciplinary Center for Clinical Research, Junior Research Group "Tumor Progression and Immune Escape", Clinics for Gynecology and Obstetrics, University of Würzburg, Würzburg, Germany

Abstract

Although glioblastomas show the same histologic phenotype, biological hallmarks such as growth and differentiation properties vary considerably between individual cases. To investigate whether different subtypes of glioblastomas might originate from different cells of origin, we cultured tumor cells from 22 glioblastomas under medium conditions favoring the growth of neural and cancer stem cells (CSC). Secondary glioblastoma (n = 7)–derived cells did not show any growth in the medium used, suggesting the absence of neural stem cell–like tumor cells. In contrast, 11/15 primary glioblastomas contained a significant CD133$^+$ subpopulation that displayed neurosphere-like, nonadherent growth and asymmetrical cell divisions yielding cells expressing markers characteristic for all three neural lineages. Four of 15 cell lines derived from primary glioblastomas grew adherently *in vitro* and were driven by CD133$^-$ tumor cells that fulfilled stem cell criteria. Both subtypes were similarly tumorigenic in nude mice *in vivo*. Clinically, CD133$^-$ glioblastomas were characterized by a lower proliferation index, whereas glial fibrillary acidic protein staining was similar. GeneArray analysis revealed 117 genes to be differentially expressed by these two subtypes. Together, our data provide first evidence that CD133$^+$ CSC maintain only a subset of primary glioblastomas. The remainder stems from previously unknown CD133$^-$ tumor cells with apparent stem cell–like properties but distinct molecular profiles and growth characteristics *in vitro* and *in vivo*. [Cancer Res 2007;67(9):4010–5]

Introduction

The differences in biology and clinical prognosis of glioblastomas suggest that glioblastomas might harbor different tumor entities arising from different cells of origin. This hypothesis is supported by controversial findings regarding the actual cell of origin of gliomas (1). Attempts to define reliable clinical, molecular, and cell biological markers that would predict individualized prognosis and allow specifically targeted therapies have been largely unsuccessful. The only established subclassification comprises primary (*de novo*) and secondary glioblastomas deriving from lower grade astrocytomas. Although both subtypes show characteristic genetic alterations, there are no clear-cut differences in terms of prognosis or response to therapy.

Recently, CD133$^+$ brain tumor–initiating cells recapitulating the original tumor *in vivo* even after serial transplantation have been described (2–6). These brain cancer stem cells (CSC) amount to 1% to 30% of a given tumor and show hallmarks of neural stem cells. They display the potential to differentiate into neuronal, astroglial, and oligodendroglial cells and, thus, sculpt the resulting tumor that comprises a characteristic mixture of different cell types. Gene expression profiling revealed that the histologically defined group of glioblastomas can be subdivided into subtypes of prognostic relevance in which gene expression profiles reflect different stages of neurogenesis (7). Consequentially, we hypothesized that different glioblastomas might go back to different CSC and, accordingly, characterized CSC from 22 glioblastomas.

Materials and Methods

Glioblastoma samples. Glioblastoma samples were provided by the local Department of Neurosurgery. Histologic analyses [Ki-67, glial fibrillary acidic protein (GFAP)] were done in the local Department of Pathology and confirmed by the German National Reference Center for Neuropathology (University of Bonn, Germany). Secondary and recurrent secondary glioblastomas were derived from lower grade astrocytomas. Experiments were approved by the local ethics committee (University of Regensburg, no. 05/105, June 14, 2005).

Culture of primary glioblastoma cells and spheres. Samples were stored in sterile saline at 4°C and processed within 24 h after resection. They were washed and dissociated by mechanical and enzymatic means. Erythrocytes were lysed using NH_4Cl. Trypan blue staining confirmed >80% viability after the procedure. Tumor cells were resuspended in DMEM-F12 containing 20 ng/mL of epidermal growth factor (EGF), basic fibroblast growth factor (bFGF; both from R&D Systems), leukemia inhibitory factor (LIF; Chemicon), and B27 (1:50; Life Technologies) as a stem cell–permissive medium.

Magnetic cell separation and fluorescence-activated cell sorting. Cells were dissociated and resuspended in PBS containing 0.5% bovine serum albumin and 2 mmol/L EDTA. For magnetic labeling, CD133/1 Micro Beads were used (Miltenyi Biotech). Positive magnetic cell separation (MACS) was done using several MACS columns in series. Cells were stained with CD133/2-PE (Miltenyi Biotech) or isotype control antibody (mIgG2b-PE, Caltag Laboratories) and analyzed on a BD FACSCalibur.

***In vivo* tumor model.** Tumor cells were suspended in 2 μL PBS and intracranially injected into T-lymphocyte–deficient NMRI$^{(nu/nu)}$ mice as described previously (2, 8). All procedures were conducted in accordance with German laws governing animal care. Tumor samples were snap frozen. Sections (10 μm) were stained with H&E using standard protocols. Antibodies (Ki-67, nestin) were purchased from Chemicon.

Immunocytochemistry. A sphere derived from one tumor cell was dissociated and stained as previously described (9). Primary antibodies used

Note: Supplementary data for this article are available at Cancer Research Online (http://cancerres.aacrjournals.org/).

Requests for reprints: Christoph P. Beier, Department of Neurology, University of Regensburg, Universitätsstrasse 84, 93053 Regensburg, Germany. Phone: 49-941-941-3258; Fax: 49-941-941-3292; E-mail: Christoph.Beier@gmx.de.

©2007 American Association for Cancer Research.

doi:10.1158/0008-5472.CAN-06-4180

Downloaded from cancerres.aacrjournals.org on June 19, 2021. © 2007 American Association for Cancer Research.

were anti–β-tubulin III (Promega), anti-GFAP (DAKO), anti-galactocerebroside C, anti-nestin, anti-NeuN, anti-Musashi (all from Chemicon), anti-doublecortin (Santa Cruz), anti-Hu (Genetex), anti-S100β (Swant), and anti-myelin basic protein. Stainings were visualized using anti-mouse Alexa Fluor 488 (Molecular Probes) or anti-rabbit–rhodamine antibody conjugates (Dianova). Nuclei were counterstained using 4′,6-diamidino-2-phenylindole (DAPI; Sigma).

Gene expression profiling. Total RNA was isolated using the Qiagen RNeasy kit. The generation of labeled cRNA and its hybridization to U133 Plus 2 GeneChip arrays (Affymetrix) were done at the Kompetenzzentrum für Fluoreszente Bioanalytik (KFB; Regensburg, Germany) according to standard procedures. Arrays were scanned on a GCS 3000 7G scanner (Affymetrix). Probe set summary and statistical data analysis were done using ArrayAssist 4.2 (Stratagene) using default parameters. Functional annotation and identification of overrepresented functional themes were done using the DAVID database.[6] Array data are available at National Center for Biotechnology Information's Gene Expression Omnibus.[7]

Results

Glioblastomas can be subclassified according to growth pattern and CD133 expression of CSC. We analyzed tumor cells from 15 primary and 7 secondary glioblastomas that had been cultured in medium promoting the growth of CSC (2, 4, 5, 7, 10–13). Fluorescence-activated cell sorting analysis of glioblastomas within 3 days after resection confirmed the presence of CD133$^+$ cells (>3%) in 14/22 samples. The relative content of CD133$^+$ cells was significantly higher in primary (n = 15) than in secondary glioblastomas (n = 7, P < 0.01; Fig. 1*A*).

After 3 to 4 weeks of primary culture, CSC cultures were characterized according to their growth pattern. Spheres derived from primary glioblastomas readily proliferated and either displayed a neurosphere-like, nonadherent growth pattern (11/15) or grew as adherent spheres (4/15) with differentiated cells in between (Fig. 1*B*). Surprisingly, CD133 expression was only associated with the neurosphere-like growing primary glioblastomas (Fig. 1*D*). Secondary glioblastomas did not form any spheres and barely proliferated (Fig. 1*C*).

CD133$^+$ CSC in primary glioblastomas. Neurosphere-like growing CD133$^+$ tumor spheres were dissociated and magnetically sorted into CD133$^+$ and CD133$^-$ cells (Fig. 2*A*; refs. 2, 8). Upon replating at 1 cell per well, only a small proportion (2–5%) of CD133$^+$ tumor cells formed spheres within 42 days, whereas no *in vitro* sphere formation was observed with CD133$^-$ cells (data not shown). Sequential minimal dilution assays for ≥3 passages confirmed that these CD133$^+$ single cell–derived tumor spheres possessed the potential to grow infinitely. The proportion of sphere-forming cells remained stable throughout the course of culture (>8 months), indicating asymmetrical cell divisions (data not shown). Cell clustering played no role in sphere formation (Fig. 2*B*). Within a single sphere grown from one CD133$^+$ CSC, cells expressed markers of all three neural lineages at constant proportion, with only few cells expressing markers of more than one lineage (Fig. 2*C*; Supplementary Fig. S1). To exclude involuntary purification of neuronal stem cells, we confirmed the morphologic hallmarks of malignancy by analyzing the nuclear morphology directly after resection and at later time points (Fig. 2*D*).

CD133$^-$ CSC in primary glioblastomas. Adherently growing tumor spheres with differentiated cells in between did not contain any CD133$^+$ tumor cells. Hence, sphere-forming and differentiating cells could not be separated by MACS (Fig. 3*A*). We therefore questioned whether these glioblastomas contained CD133$^-$ CSC. Using the minimal dilution assay, we found that only 0.5% to 2% of

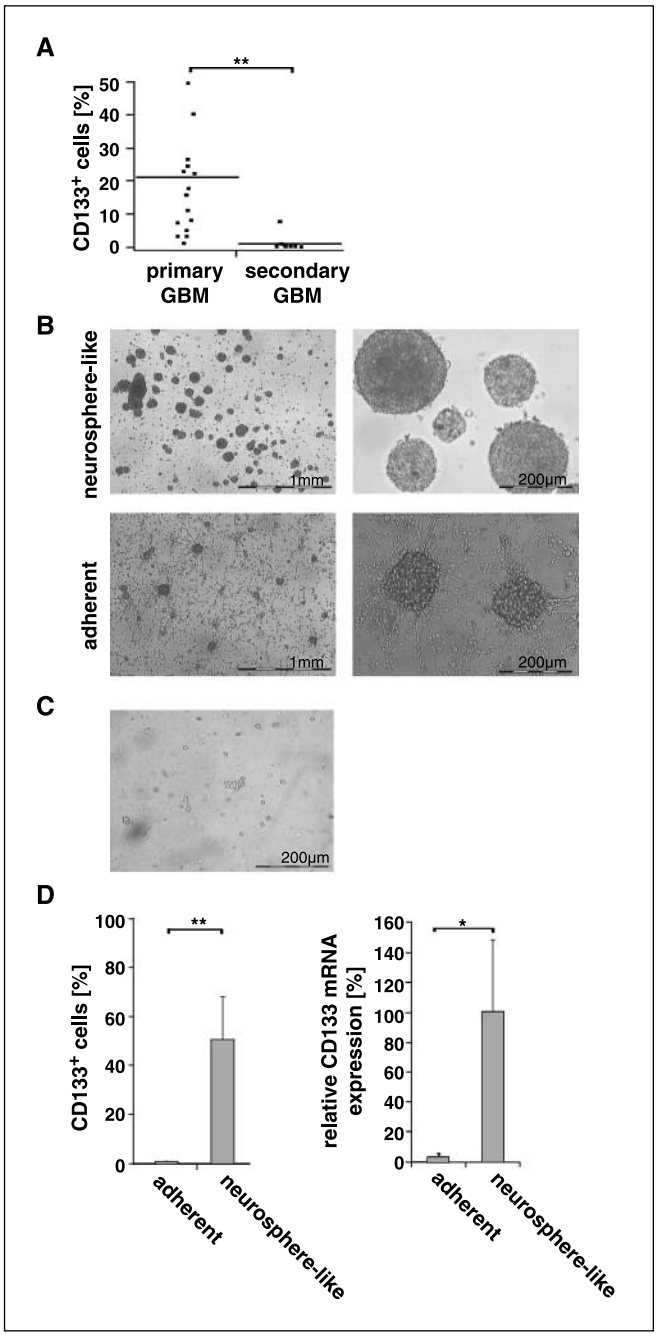

Figure 1. Glioblastomas can be subclassified according to growth pattern and CD133 expression of CSC. *A,* flow cytometry was used to determine the proportion of CD133-positive cells from primary (15/22) and secondary (7/22) glioblastomas. Cells were analyzed within 3 d of primary *in vitro* culture. *B* to *D,* after 3 to 4 wks of primary culture, CSC lines were characterized according to their growth pattern and CD133 expression. *B,* neurosphere-like nonadherent (*top*, 11/15 glioblastomas) and adherent (*bottom*, 4/15 glioblastomas) growth patterns observed in primary glioblastomas. *C,* secondary and recurrent secondary glioblastomas showed neither sphere formation nor tumor cell growth. *D,* flow-cytometric determination of the percentage of CD133-positive cells in adherently and neurosphere-like growing primary glioblastomas and relative expression of CD133-mRNA. *, P = 0.05; **, P = 0.01, Student's t test. *Columns,* mean; *bars,* SE.

[6] http://david.abcc.ncifcrf.gov/home.jsp
[7] http://www.ncbi.nlm.nih.gov/geo

Downloaded from cancerres.aacrjournals.org on June 19, 2021. © 2007 American Association for Cancer Research.

replated tumor cells were able to proliferate and form new adherent spheres (Supplementary Fig. S2). However, sequential minimal dilution assays showed that this small subset of cells could be propagated for ≥3 passages while retaining their phenotype (data not shown). Within the CD133⁻ CSC-derived tumor spheres, differentiated cells expressing markers from all three neural lineages could be found. Only few cells were positive for more than one marker, indicating transient states of differentiation (Fig. 3*B*, Supplementary Fig. S1).

This confirms that also a small subset of CD133⁻ glioblastoma cells can undergo asymmetrical cell divisions, differentiate, and maintain infinite growth potential. Accordingly, we consider these cells to be yet uncharacterized CD133⁻ CSC that may be specific for a novel subtype of glioblastomas.

***In vivo* tumorigenicity of CD133⁺ and CD133⁻ CSC.** When 10^5 or 10^6 tumor cells of a CD133⁻ CSC line were implanted into immunodeficient nude mice (n = 6), large glioblastoma-like lesions formed within 50 days (Fig. 3*C*). Although CD133⁺ cells from CD133⁺ CSC lines were similarly tumorigenic, no tumors were formed by CD133⁻ cells from CD133⁺ CSC cell lines (n = 6).

To study possible clinical differences between CD133⁻ and CD133⁺ CSC, the histologic properties of the original glioblastomas were analyzed, revealing that glioblastomas containing CD133⁻ CSC showed a significantly lower proliferation index (Ki-67) than CD133⁺ glioblastomas (Fig. 3*D*), but similar GFAP expression (data not shown).

Gene expression profiling of CD133⁺ and CD133⁻ CSC lines derived from primary glioblastomas. To determine differentially expressed genes, we used Affymetrix U133 2.0 Plus arrays to compare the genome-wide expression patterns of three CD133⁻ and three CD133⁺ CSC lines. To generate a list of probe sets that differentiate the two groups, both MAS5 and GC-RMA raw signals were calculated. The MAS5 Detection Call was used to remove probe sets that were called A on all six arrays. Probe sets with signal values below 20 for all six arrays were not used for downstream analysis. Genes were considered as differentially expressed if the log 2 signals differed significantly (t test, $P < 0.05$), and the average ratio of log 2 signals was at least 2. This strategy yielded sets of 383 (MAS5) or 321 (GC-RMA) probe sets, respectively (Supplementary Figs. S1 and S2). The intersection of the two lists consists of 117 genes, including CD133 (Table 1 and Supplementary Fig. S3). The most striking difference was the up-regulated expression of seven MHC class II proteins in CD133⁻ cell lines.

No CSC cultures could be derived from secondary glioblastomas. Secondary glioblastomas (7/22) were found to contain hardly any CD133⁺ cells (Fig. 1*A*). Having found that the chosen culture conditions were permissive for CD133⁻ CSC, we attempted to grow cells from secondary glioblastomas (7/22). Surprisingly, neither sphere formation nor significant *in vitro* growth was observed (Fig. 1*C*), although cells were >80% viable, as judged by trypan blue exclusion. The cancerous nature of the nonproliferating cells was confirmed by DAPI staining (data not shown). Because three recurrent primary glioblastomas showed neurosphere-like growth and CD133 expression, the different behavior of secondary glioblastomas is not likely due to previous therapy, but rather to different characteristics of the cells that initiated the original lower grade astrocytomas (data not shown).

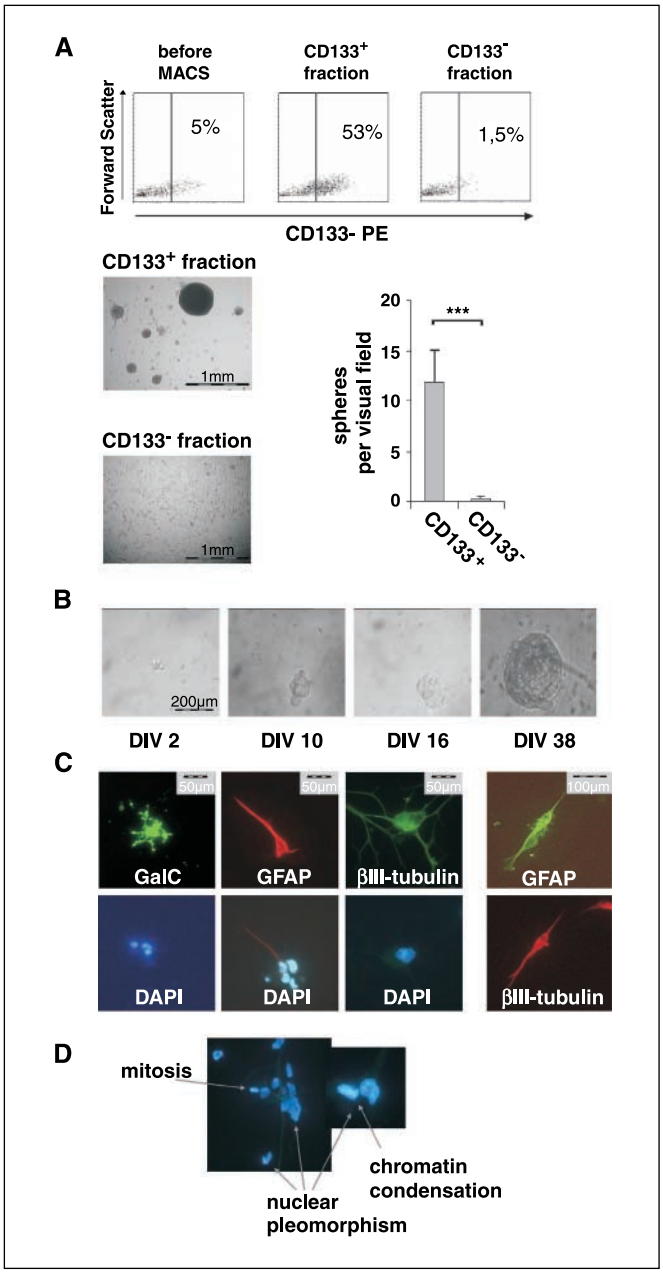

Figure 2. CD133⁺ CSC in primary glioblastomas. After 3 to 4 wks of primary cell culture, 11/15 CSC lines derived from primary glioblastomas were characterized by neurosphere-like, nonadherent growth and expression of CD133. *A,* CD133⁺ tumor cells were separated using MACS, and purity was assessed by flow cytometry. CD133⁺ and CD133⁻ tumor cells were plated separately into a 96-well plate at 100 cells per well. After 21 d, the number of spheres was counted in 30 wells. ***, $P < 0.001$, Student's t test. *Column,* mean; *bar,* SE. *B,* photographs of a representative sphere taken at 2, 10, 16, and 38 d of culture. *DIV,* days *in vitro*. *C,* a sphere derived from a single CD133⁺ cell was dissociated, and cells were stained for markers of the three neural lineages and with DAPI. *GalC,* oligodendroglial; *GFAP,* astroglial; *βIII-tubulin,* neuronal; *DAPI,* nuclear staining. A few cells were positive for the neuronal (β-tubulin) and glial marker (GFAP, *right*). *D,* nuclei from cells that had grown in glioblastoma-derived spheres were stained with DAPI to reveal altered nuclear morphologies. Representative nuclei showing hallmarks of malignancy like frequent mitoses, chromatin condensation, and nuclear pleomorphism are shown.

Discussion

Confirming previous reports, cell lines derived from CD133⁺ CSC showed neurosphere-like growth (2–5, 10, 11). However, some primary glioblastoma cell lines grew as adherent spheres within a dense network of differentiated cells and were maintained by

Downloaded from cancerres.aacrjournals.org on June 19, 2021. © 2007 American Association for Cancer Research.

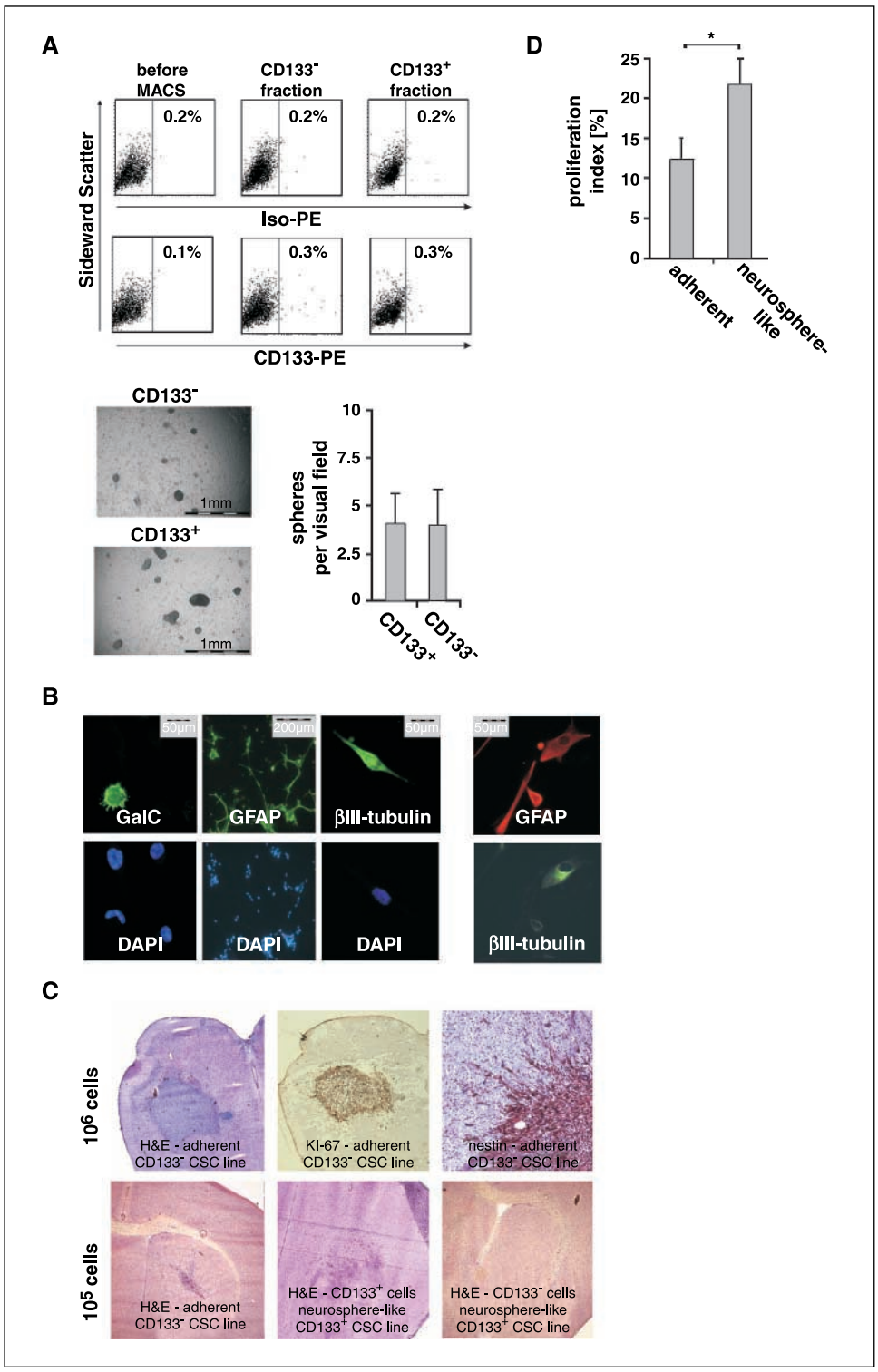

Figure 3. CD133⁻ CSC in primary glioblastomas. *A,* after 3 to 4 wks of primary culture, CD133⁻ CSC were detected in CSC lines of primary glioblastomas (4/15) showing adherent growth. No separation into different fractions was achieved by MACS for CD133⁺ cells. Nor were CD133-expressing cells detectable by flow-cytometric analysis. *B,* a tumor sphere derived from a single CD133⁻ tumor cell was dissociated, and cells were stained for markers of all three neural lineages. A subset of cells was positive for more than one marker protein (*right*). *C,* to show the tumorigenicity of CD133⁻ CSC, 10^6 cells were injected into the brains of nude mice, and the tumor size was analyzed after 50 d. Tumors showed strong positivity for Ki-67 and nestin (*top*). For a more detailed comparison of the respective tumorigenicity, mice were intracranially injected with either 10^5 cells of an adherently growing CD133⁻ CSC line or with 10^5 magnetically sorted CD133⁺ or CD133⁻ cells from a neurosphere-like growing CD133⁺ CSC line. The entire brains were analyzed using H&E staining every 100 µm; representative figures are shown (*bottom*). *D,* paraffin-embedded sections from tumors that had given rise to neurosphere-like growing CD133⁺ CSC lines or to adherently growing CD133⁻ CSC lines were stained with anti–Ki-67 antibody. The proliferation index was determined by counting the percentage of Ki-67–positive cells. *, $P < 0.05$, Student's *t* test. *Columns,* mean; *bars,* SE.

CD133⁻ cells that display infinite potential for self-renewal. Pluripotency was confirmed by expression of neuronal, astrocytic, and oligodendroglial lineage markers (Figs. 2*C* and 3*B* and Supplementary Fig. S1) in daughter cells. The question whether CSC-derived differentiated cells could actually fulfill neuronal, astrocytic, or oligodendroglial functions has not been addressed. Considering their frequent mitoses, chromatin condensation, atypical nuclei, and other hallmarks of cancer, they are unlikely to assume any useful function in the healthy brain. To confirm that the small subpopulation of CD133⁻ tumor cells is rightly referred to as CSC, evidence for their selective capability to drive tumor growth *in vivo* is needed. Because there is no surface marker allowing the separation of CD133⁻ CSC from CD133⁻ cells lacking stem cell properties, experiments similar to those done with the purified CD133⁺ CSC subset (2) are not feasible yet. The observation that adherent CD133⁻ cell cultures are tumorigenic

Downloaded from cancerres.aacrjournals.org on June 19, 2021. © 2007 American Association for Cancer Research.

Table 1.

Affymetrix ID	Fold up-regulation	Gene name
(A) Selection of genes up-regulated in CD133$^+$ CSC lines		
Growth factors/intracellular signaling		
212448_at	4.6	Neural precursor cell expressed
227449_at	4.5	EPH receptor A4
226974_at	4.4	Neural precursor cell expressed
204379_s_at	4.0	Fibroblast growth factor receptor 3
227542_at	2.0	Suppressor of cytokine signaling 6
Neuronal proteins/neuronal progenitors		
206633_at	20.4	Cholinergic receptor
204304_s_at	19.0	CD133/prominin 1
216086_at	6.0	Synaptic vesicle glycoprotein 2C
DNA interacting proteins/transcription factors		
230785_at	9.5	Sal-like 3
228347_at	3.5	Sine oculis homeobox homologue 1
203604_at	2.5	Zinc finger protein 516
203221_at	2.3	Transducin-like enhancer of split 1
229123_at	2.2	Zinc finger protein 224
Migration and extracellular matrix–associated genes		
204724_s_at	10.9	Collagen, type IX, α 3
203413_at	10.3	NEL-like 2
(B) Selection of genes up-regulated in CD133$^-$ CSC lines		
Immune system		
212998_x_at	44.9	MHC, class II, HLA-DQ β1
213831_at	36.1	MHC, class II, HLA-DQ α1
215193_x_at	21.2	MHC, class II, HLA-DR β1
208306_x_at	16.9	MHC, class II, HLA-DR α
211991_s_at	12.3	MHC, class II, HLA-DP α1
1567628_at	9.6	CD74 antigen
217478_s_at	8.1	MHC, class II, HLA-DM α
203932_at	4.9	MHC, class II, DM β
Growth factors/receptors/intracellular signaling		
203987_at	26.6	Frizzled homologue 6
205290_s_at	5.6	Bone morphogenetic protein 2
208712_at	5.3	Cyclin D1
38037_at	3.3	Heparin-binding EGF-like growth factor
210095_s_at	2.8	Insulin-like growth factor binding protein 3
202794_at	2.7	Inositol polyphosphate-1-phosphatase
217717_s_at	2.4	Tyrosine 3-monooxygenase activation protein
201537_s_at	2.3	Dual-specificity phosphatase 3
211665_s_at	2.0	Son of sevenless homologue 2
209311_at	2.0	BCL2-like 2
219483_s_at	2.0	Porcupine homologue
Neuronal proteins/neuronal progenitors		
202391_at	61.3	Brain-abundant, membrane-attached signal protein 1
210770_s_at	3.9	Voltage-dependent calcium channel (P/Q type, α 1A subunit)
DNA interacting proteins/transcription factors		
227705_at	3.8	Transcription elongation factor A (SII)-like 7
223603_at	3.7	Zinc finger protein 179
225941_at	3.4	Eukaryotic translation initiation factor 4E member 3
229412_at	3.4	Taube nuss homologue
213189_at	2.7	MYC induced nuclear antigen
229986_at	2.3	Kruppel-like zinc finger factor X17
59999_at	2.3	Hypoxia-inducible factor 1, α subunit inhibitor
206472_s_at	2.2	Transducin-like enhancer of split 3/Esp1 homologue
1555420_a_at	2.1	Kruppel-like factor 7
Migration and extracellular matrix–associated genes		
203167_at	3.1	Tissue inhibitor of metalloproteinase metallopeptidase inhibitor 2
229689_s_at	2.3	Discs, large homologue 5

Downloaded from cancerres.aacrjournals.org on June 19, 2021. © 2007 American Association for Cancer Research.

in vivo, whereas CD133$^-$ cells from neurosphere-like CD133$^+$ CSC lines do not form tumors in nude mice (Fig. 3*C*), is the strongest currently obtainable evidence for the existence of CD133$^-$ CSC consequently referred to as CD133$^-$ CSC. Because only the total number of adherent CD133$^-$ cells injected into immunodeficient mice is known, we cannot determine how many CD133$^-$ CSC are required to induce tumor formation *in vivo*.

GeneArrays unveiled a multitude of differentially regulated genes between CD133$^-$ and CD133$^+$ CSC lines. CD133$^-$ CSC lines expressed MHC class II encoding genes that have not been described in glioblastomas and might be exploited for tumor immunotherapy. *In vivo*, CD133$^+$ glioblastomas differ through a higher proliferation index, indicating a possible prognostic significance. The combination of molecular differences and different biological growth patterns *in vitro* and *in vivo* suggest that CD133$^+$ and CD133$^-$ CSC lines might reflect two biologically different glioblastoma subtypes. The respective primary glioblastomas might arise from different cells of origin or from related cell types having acquired different molecular alterations.

Secondary and primary glioblastomas are well-established entities defined by the clinical course of the disease. They have a common histologic phenotype but differ on a molecular level (14). These molecular differences are clearly reflected by different characteristics of their respective CSC *in vitro*. Due to neurosphere-like morphology and the strong expression of CD133 observed with CSC from one subtype of primary glioblastomas, their cells of origin might be neural stem cells (1, 15–17). CSC from secondary glioblastomas did not grow under conditions suitable for the culture of neural stem cells, suggesting that the putative CSC may be derived from a different cell of origin. In fact, a "proneural" subtype characterized by a neuroblast-like expression pattern, the lack of CD133 expression, and the failure to grow in media containing EGF and bFGF has been reported recently (7).

Taken together, our data show that there are at least two different types of CSC in primary glioblastomas, which can be characterized *in vitro* under conditions suitable for the culture of neural stem cells, whereas no stem cell–like cells could be derived from secondary glioblastomas. We therefore suggest that primary glioblastomas should be further subclassified according to the properties of their CSC. Knowing the cells that drive a given tumor, and possibly their cell of origin, may help to devise novel and specific treatment strategies.

Acknowledgments

Received 11/16/2006; revised 3/1/2007; accepted 3/19/2007.

Grant support: ReForM program of the University of Regensburg (D. Beier and C.P. Beier) and BayGene (P.J. Oefner).

The costs of publication of this article were defrayed in part by the payment of page charges. This article must therefore be hereby marked *advertisement* in accordance with 18 U.S.C. Section 1734 solely to indicate this fact.

References

1. Fan X, Salford LG, Widegren B. Glioma stem cells: evidence and limitation. Semin Cancer Biol 2007;17:214–8.
2. Singh SK, Hawkins C, Clarke ID, et al. Identification of human brain tumour initiating cells. Nature 2004;432:396–401.
3. Galli R, Binda E, Orfanelli U, et al. Isolation and characterization of tumorigenic, stem-like neural precursors from human glioblastoma. Cancer Res 2004;64:7011–21.
4. Hemmati HD, Nakano I, Lazareff JA, et al. Cancerous stem cells can arise from pediatric brain tumors. Proc Natl Acad Sci U S A 2003;100:15178–83.
5. Yuan X, Curtin J, Xiong Y, et al. Isolation of cancer stem cells from adult glioblastoma multiforme. Oncogene 2004;23:9392–400.
6. Reya T, Morrison SJ, Clarke MF, Weissman IL. Stem cells, cancer, and cancer stem cells. Nature 2001;414:105–11.
7. Phillips HS, Kharbanda S, Chen R, et al. Molecular subclasses of high-grade glioma predict prognosis, delineate a pattern of disease progression, and resemble stages in neurogenesis. Cancer Cell 2006;9:157–73.
8. Bao S, Wu Q, McLendon RE, et al. Glioma stem cells promote radioresistance by preferential activation of the DNA damage response. Nature 2006;444:756–60.
9. Wachs FP, Couillard-Despres S, Engelhardt M, et al. High efficacy of clonal growth and expansion of adult neural stem cells. Lab Invest 2003;83:949–62.
10. Singh SK, Clarke ID, Terasaki M, et al. Identification of a cancer stem cell in human brain tumors. Cancer Res 2003;63:5821–8.
11. Ignatova TN, Kukekov VG, Laywell ED, Suslov ON, Vrionis FD, Steindler DA. Human cortical glial tumors contain neural stem-like cells expressing astroglial and neuronal markers *in vitro*. Glia 2002;39:193–206.
12. Kondo T, Setoguchi T, Taga T. Persistence of a small subpopulation of cancer stem-like cells in the C6 glioma cell line. Proc Natl Acad Sci U S A 2004;101:781–6.
13. Lee J, Kotliarova S, Kotliarov Y, et al. Tumor stem cells derived from glioblastomas cultured in bFGF and EGF more closely mirror the phenotype and genotype of primary tumors than do serum-cultured cell lines. Cancer Cell 2006;9:391–403.
14. Kleihues P, Ohgaki H. Primary and secondary glioblastomas: from concept to clinical diagnosis. J Neurooncol 1999;1:44–51.
15. Uhrbom L, Dai C, Celestino JC, Rosenblum MK, Fuller GN, Holland EC. Ink4a-Arf loss cooperates with KRas activation in astrocytes and neural progenitors to generate glioblastomas of various morphologies depending on activated Akt. Cancer Res 2002;62:5551–8.
16. Fomchenko EI, Holland EC. Stem cells and brain cancer. Exp Cell Res 2005;306:323–9.
17. Uchida N, Buck DW, He D, et al. Direct isolation of human central nervous system stem cells. Proc Natl Acad Sci U S A 2000;97:14720–5.

Downloaded from cancerres.aacrjournals.org on June 19, 2021. © 2007 American Association for Cancer Research.

Cancer Research
The Journal of Cancer Research (1916–1930) | The American Journal of Cancer (1931–1940)

AACR American Association for Cancer Research

CD133^{+} and CD133^{-} Glioblastoma-Derived Cancer Stem Cells Show Differential Growth Characteristics and Molecular Profiles

Dagmar Beier, Peter Hau, Martin Proescholdt, et al.

Cancer Res 2007;67:4010-4015.

Updated version	Access the most recent version of this article at: http://cancerres.aacrjournals.org/content/67/9/4010
Supplementary Material	Access the most recent supplemental material at: http://cancerres.aacrjournals.org/content/suppl/2007/04/30/67.9.4010.DC1

Cited articles	This article cites 17 articles, 6 of which you can access for free at: http://cancerres.aacrjournals.org/content/67/9/4010.full#ref-list-1
Citing articles	This article has been cited by 82 HighWire-hosted articles. Access the articles at: http://cancerres.aacrjournals.org/content/67/9/4010.full#related-urls

E-mail alerts	Sign up to receive free email-alerts related to this article or journal.
Reprints and Subscriptions	To order reprints of this article or to subscribe to the journal, contact the AACR Publications Department at pubs@aacr.org.
Permissions	To request permission to re-use all or part of this article, use this link http://cancerres.aacrjournals.org/content/67/9/4010. Click on "Request Permissions" which will take you to the Copyright Clearance Center's (CCC) Rightslink site.

Downloaded from cancerres.aacrjournals.org on June 19, 2021. © 2007 American Association for Cancer Research.